Neoplasma 2024; 71(3): 266–278

doi:10.4149/neo_2024_231006N524

ARTN-GFRA3 axis induces epithelial-mesenchymal transition phenotypes, migration, and invasion of gastric cancer cells via KRAS signaling

Xiao-Long WANG[1,2], Gui-Xiu JIN[3], Xiao-Qiang DONG[1,*]

[1]Department of General Surgery, The First Affiliated Hospital of Soochow University, Suzhou, Jiangsu, China; [2]Department of General Surgery, Taixing People's Hospital, Taizhou, Jiangsu, China; [3]Department of Obstetrics and Gynecology, Taixing People's Hospital, Taizhou, Jiangsu, China

**Correspondence: dongxq@hotmail.com*

Received October 6, 2023 / Accepted June 10, 2024

Neural invasion underlies the local spread of gastric cancer and is associated with poor prognosis. This process has been receiving increasing attention in recent years. However, the relationship between neural invasion and the malignant phenotypes of gastric cancer cells, as well as the molecular mechanism involved in this process, remain unclear. In this study, bioinformatics analysis was performed using a dataset obtained from The Cancer Genome Atlas-Stomach Adenocarcinoma. The results revealed that high expression of GDNF family receptor alpha 3 (GFRA3) was associated with a poor prognosis of patients with gastric cancer. GFRA3 is a receptor for artemin (ARTN), a glial cell line-derived neurotrophic factor (GDNF). This association was indicated by short overall/disease-free survival, as well as the presence of high-stage and high-grade disease. Gene set enrichment analysis showed that two cancer-associated pathways, namely KRAS signaling and epithelial-mesenchymal transition (EMT), were activated when GFRA3 was highly expressed in gastric cancer. Further studies confirmed that GFRA3 activated KRAS downstream signaling phosphatidylinositol 3 kinase/protein kinase B (PI3K/AKT) or extracellular signal-regulated kinase (ERK) and induced EMT markers, as well as promoted the migration and invasion of gastric cancer cells. As a ligand of GFRA3, ARTN induced the EMT, migration, and invasion of gastric cancer cells via GFRA3. Notably, the effects of the ARTN-GFRA3 axis were attenuated by treatment with a KRAS inhibitor. The present findings indicated that, during the neural invasion of gastric cancer, ARTN-mediated activation of GFRA3 induces EMT phenotypes, migration, and invasion of gastric cancer cells via KRAS signaling.

Key words: neural invasion; GFRA3; ARTN; KRAS signaling; epithelial-mesenchymal transition

In recent years, gastric cancer has become the fifth common type of malignant tumors, with >1 million new cases reported each year worldwide. This disease is often diagnosed at an advanced stage, rendering it the third leading cause of cancer-associated mortality [1]. Neural invasion was found in approximately 35.9% of patients with gastric cancer during the postoperative pathological diagnosis [2]. During their growth, cancer cells surround the nerves (at least one-third of the perimeter) or invade any outer membranes of the nerves (e.g., epineurium, perineurium, and endoneurium) [3]. Neural invasion is associated with poor prognosis of various types of cancer, including gastric cancer. It has been demonstrated that neural invasion is a reliable factor for predicting the survival outcome of patients with gastric cancer [2, 4–6]. Therefore, it is of great significance to reveal the molecular mechanism underlying neural invasion in gastric cancer.

Members of the GDNF family receptor alpha (GFRA) family are the receptors for glial cell line-derived neurotrophic factors (GDNFs), including GDNF, neurturin (NRTN), persephin (PSPN), and artemin (ARTN), which comprise GFRA1-4 [7]. The GDNF-GFRA complex subsequently binds to and activates the transmembrane RET receptor tyrosine kinase, which transduces cellular signaling [8]. The ARTN-GFRA3 axis plays important roles in a variety of physiological functions, including the development and maintenance of various neuronal populations, neurite growth, and nerve regeneration. However, it is also required for tumor development. Increased GFRA3 expression is significantly correlated with poor prognosis of patients with breast cancer and urothelial cancer [9, 10]. Moreover, GFRA3 plays an essential role in the neuroinfiltration and metastasis of pancreatic cancer; hence, it can serve as an indicator of

the biological behavior of pancreatic cancer [11]. Thus far, the prognostic significance and biological role of GFRA3 in gastric cancer have not been reported.

As a biological process, epithelial–mesenchymal transition (EMT) triggers the detachment of polarized epithelial cells from neighboring cells and transforms them into mesenchymal cells. In tumor cells, EMT leads to loss of epithelial polarity and induces their transformation into mesenchymal phenotypes, thereby playing a critical role in tumor invasion and metastasis [12]. Evidence has shown that the over activated EMT is closely related to the occurrence, invasion, and metastasis of gastric cancer [13, 14]. Tumor metastasis is a complex process, mainly including local invasion, intravasation, metastasis, and extravasation. Malignant cells leave the primary site, colonize tissues, and form secondary tumors in neighboring or distant organs, thus causing gastric cancer-associated death [15]. The mesenchymal phenotype is linked to a higher risk of invasion and metastasis than the intestinal phenotype, which is mainly present in early-stage gastric cancer [16]. Moreover, gastric cancer with EMT molecular phenotype is typically associated with advanced disease and indicates a poor prognosis [17]. Therefore, investigating the mechanisms of EMT in gastric cancer may help understand the invasion and metastasis of this malignancy.

In the present study, a bioinformatics analysis based on data obtained from The Cancer Genome Atlas (TCGA) database suggested that high expression of GFRA3 was associated with a poor prognosis of patients with gastric cancer. Furthermore, it was found that the ARTN-GFRA3 axis induced EMT, and promoted the migration and invasion of gastric cancer cells through activation of KRAS signaling. Clinical analysis also revealed a relationship between GFRA3 expression and the TNM stage of gastric cancer.

Materials and methods

Data acquisition. RNA-sequencing data and clinical follow-up information were obtained from TCGA database (https://www.genome.gov/Funded-Programs-Projects/Cancer-Genome-Atlas). The datasets included glioblastoma, uterine corpus endometrial carcinoma, kidney renal papillary cell carcinoma (KIRP), colon adenocarcinoma (COAD), thyroid carcinoma, lung adenocarcinoma (LUAD), bladder urothelial carcinoma (BLCA), liver hepatocellular carcinoma (LIHC), stomach adenocarcinoma (STAD), head and neck squamous cell carcinoma (HNSC), lung squamous cell carcinoma, esophageal carcinoma (ESCA), cervical squamous cell carcinoma (CESC), cholangiocarcinoma, rectum adenocarcinoma (READ), prostate adenocarcinoma (PRAD), pancreatic adenocarcinoma, breast invasive carcinoma, kidney renal clear cell carcinoma, and kidney chromophobe. The expression of GFRA3 in all tumors was evaluated as transcripts per million in the mRNA-sequencing data. The optimal cutoff value was determined using the R package "survminer". Patients were classified into high- and low-expression groups based on the levels of GFRA3.

The study was conducted in accordance with the Declaration of Helsinki, and approved by the Ethics Committee of the National Human Genetic Resources Sharing Service Platform (grant number: SHYJS-CP-1410012). Informed consent was obtained from all subjects involved in the study.

Prognostic analysis. The R package "survminer" and "survival" were used to generate Kaplan-Meier curves of overall survival (OS) and disease-free survival (DFS) based on the expression of GFRA3 for each cancer type. The significance of differences in OS and DFS between the groups with high and low expression of GFRA3 was evaluated using the log-rank test.

Expression analysis of GFRA3 in the pan-cancer setting. The expression levels of GFRA3 in normal and tumor tissues were compared and illustrated using a box plot. The expression levels of GFRA3 in the different stages and grades of the STAD dataset were compared using UALCAN (http://ualcan.path.uab.edu/analysis. html).

Gene set enrichment analysis (GSEA) analysis of GFRA3 in the pan-cancer setting. The GSEA algorithm in combination with the hallmark gene set in the R-package cluster profiler (latest version) was used to calculate the GSEA score for each functional gene set in each tumor type. Next, the Pearson correlation coefficient was used to calculate the correlation between GFRA3 expression and each functional gene set; the correlation matrix was displayed using a heat map. Based on correlation coefficients and statistical significance ($p<0.05$), the functional gene sets that were significantly correlated with GFRA3 were identified in each cancer type. The GSEA scores of the identified gene sets in tumor and adjacent normal tissues of each type of cancer were compared using a paired t-test.

Cell culture, transfection, and treatment. Human gastric cancer cell lines SGC7901 and BGC823 were purchased from the American Type Culture Collection (Manassas, VA, USA). These cells were cultured in RPMI-1640 medium containing 10% fetal bovine serum (Gibco; Thermo Fisher Scientific, Inc., Waltham, MA, USA) in an incubator at 37 °C with 5% CO_2. GFRA3 overexpression plasmids and small-interfering RNAs (siRNAs) were transfected using Lipofectamine™ 2000 (Invitrogen; Thermo Fisher Scientific, Inc.) according to the instructions provided by the manufacturer. ARTN (20 ng/ml) (P00854-10 μg; Solarbio, Beijing, China) and KRAS inhibitor BAY-293 (50 nM, S8826; Selleck, Houston, TX, USA) were used to treat SGC7901 and BGC823 cells.

Plasmids, siRNAs, and antibodies. GFRA3 overexpression plasmids were constructed based on pcDNA3.1. The siRNAs targeting GFRA3 were synthesized from GenePharma (Shanghai, China). Antibodies against GFRA3 (25379-1-AP), KRAS (12063-1-AP), phosphorylated-protein kinase B (p-AKT; 28731-1-AP), AKT (10176-2-AP), phosphory-

lated-Extracellular Signal-Regulated kinase 1/2 (p-ERK1/2; 28733-1-AP), ERK1/2 (11257-1-AP), E-cadherin (20874-1-AP), Zona occludens 1 (ZO-1; 21773-1-AP), Vimentin (VIM; 10366-1-AP), and Fibronectin (FN; 15613-1-AP) were purchased from Proteintech (Rosemont, PA, USA). The antibody against Glyceraldehyde-3-Phosphate Dehydrogenase (GAPDH; #5174) was purchased from Cell Signaling Technology (CST, Beverly, MA, USA).

Quantitative polymerase chain reaction (qPCR). According to the instructions provided by the manufacturer, total RNA was isolated from SGC7901 and BGC823 cells using RNAiso Plus (Takara Bio, Inc., Otsu, Japan). RNA quality and concentration were measured by a NanoDrop ND-1000 spectrophotometer (Thermo, Waltham, MA, USA). RNA (500 ng) was reverse-transcribed using a cDNA Reverse Transcription kit (Takara Bio, Inc.) according to the instructions provided by the manufacturer. The obtained cDNAs were analyzed in triplicate using qPCR (95 °C for 5 min, followed by 40 cycles of 95 °C for 45 s, annealing at 55 °C for 45 s, and extension at 72 °C for 1 min) on an ABI 7500 (Applied Biosystems, Carlsbad, CA, USA) with SYBR Premix Ex Taq (MX200017; Meixuan, Shanghai, China), according to the instructions provided by the manufacturer. The expression levels of target genes were normalized to those of GAPDH (internal control) and calculated using the $2^{-\Delta\Delta Ct}$ method. The sequences of the qPCR primers used in this study are listed in Table 1.

Western blotting. Cells were harvested and lysed using radioimmunoprecipitation assay lysis buffer (P0013; Beyotime, Shanghai, China). The protein concentration was determined using the BCA Protein Quantitation Kit (P0010; Beyotime). The proteins (40 μg/lane) were separated by sodium dodecyl sulfate-polyacrylamide gel electrophoresis (10%) and transferred onto polyvinylidene difluoride membrane (IPVH00010; Millipore, Temecula, CA, USA). The membrane was blocked with 5% bovine serum albumin (diluted in Tris-buffered saline with Tween-20) for 2 h at room temperature. Subsequently, the membrane was incubated with diluted primary antibodies at 4 °C overnight. This was followed by incubation with horseradish peroxidase-labeled sheep anti-rabbit secondary antibody (1:500; Jackson Immuno Research Laboratories, Inc., PA, USA) and/or horseradish peroxidase-labeled sheep anti-mouse secondary antibody (1:500; Jackson Immuno Research Laboratories, Inc.) for 2 h. The polyvinylidene difluoride membrane was immersed in chemiluminescence detection reagent for 2 min, and proteins were detected through enhanced chemiluminescence (WBKLS0500; Millipore).

Table 1. The sequences of the qPCR primers.

Gene	Forward primer	Reverse primer
GFRA3	CCCGCAGCCTTGGTAACTAT	GCCGGTCACACTTGTCATTG
GAPDH	GCACCGTCAAGGCTGAGAAC	TGGTGAAGACGCCAGTGGA

Cell Counting Kit-8 assay. SGC7901 and BGC823 cells were detached with trypsin and reseeded at a density of 5×10^4 cells/ml. A cell suspension (100 μl) was prepared in a 96-well plate, which was placed in an incubator at 37 °C with 5% CO_2 for 24 h. After culture, Cell Counting Kit-8 solution (C0037; Beyotime) (10 μl) was added to each well. The plate was incubated for 1–3 h. The absorbance at 450 nm was measured using an automatic plate reader (MULTISKAN MK3; Thermo Fisher Scientific, Inc.).

Transwell assay. SGC7901 and BGC823 cells were detached with trypsin and reseeded at a density of 5×10^5/ml. A total of 5×10^4 cells (100 μl of cell suspension) were inoculated in the Transwell chamber coated without or with Matrigel for the migration and invasion assay (BD, Franklin Lake, NJ, USA), respectively. Fresh medium containing 20% fetal bovine serum (500 μl) was added to the lower chamber, and the cells were cultured in an incubator at 37 °C with 5% CO_2 for 24 h. Thereafter, the Transwell chamber was removed, and the unmigrated cells were carefully discarded with a cotton swab. The migrated cells were fixed with 4% paraformaldehyde for 10 min, dyed with crystal violet solution for 5 min, and washed with phosphate-buffered saline. The numbers of migrated cells were counted under a microscope.

Immunohistochemical analysis. After obtaining informed consent from all patients, gastric cancer samples were collected from the National Human Genetic Resources Sharing Service Platform (2005DKA21300). Immunohistochemistry was performed using the EnVision detection system (Dako, Carpinteria, CA, USA) according to the manufacturer's instructions. To assess the score for each slide, eight 200× fields were selected, and 100 cancer cells were counted in each field. Immunostaining intensity was divided into four grades: 0, negative; 1, weak; 2, gentle; and 3, strong. The proportions of positively stained cells were classified into five grades: 0, <25%; 1, 25–50%; 2, 50–75%; 3, >75%. Staining results were evaluated and confirmed by two independent investigators blinded to the clinical data. The positive rate of tumor cells and staining intensity were multiplied to acquire IHC scores. Scores 0 were defined as –, 1–3 as +, 4–6 as ++, and 7–9 as +++. Cases with inconsistent scores were further discussed to reach a consensus.

Statistical analysis. The statistical analysis was performed using SPSS 22.0 (IBM Corp., Armonk, NY, USA) and GraphPad Prism 5.0 (GraphPad Software Inc., San Diego, CA, USA). The results are presented as the mean ± standard deviation of three separate experiments. Statistical data analysis involved the two-tailed Student's t-test, one-way analysis of variance, and chi-squared test. OS was analyzed using Kaplan-Meier plots and log-rank tests. A paired t-test was used to compare the GSEA scores in tumor and adjacent normal tissues. χ^2 test or Fisher's exact probability test was used to compare the clinicopathological features of patients with GFRA3 expression. P-values <0.05 indicate statistically significant differences.

Results

Association of GFRA3 expression with prognosis in the pan-cancer setting. To investigate the association of GFRA3 expression with prognosis in different types of cancer, TCGA datasets for 20 malignancies were analyzed. The OS analysis showed that high expression of GFRA3 was significantly associated with poor prognosis in the BLCA, KIRP, LIHC, and STAD datasets. In contrast, high GFRA3 expression was linked to a better prognosis in the PRAD and LUAD datasets (Figure 1). Next, we investigated whether GFRA3 affects the DFS in different types of cancer. As shown in Figure 2, high expression of GFRA3 was significantly associated with shorter DFS in the BLCA, COAD, ESCA, KIRP, LIHC, and STAD datasets, but longer DFS in the HNSC and PRAD datasets. Notably, the differences in both OS and DFS were significant in STAD with high and low expression of GFRA3, suggesting an important prognostic value of GFRA3 in gastric cancer.

Expression analysis of GFRA3 in the STAD dataset. The expression of GFRA3 in the pan-cancer setting and normal tissues was analyzed using TCGA datasets. The analysis demonstrated that the expression of GFRA3 was lower in most cancer tissues versus normal tissues (Figure 3A). Although GFRA3 expression was downregulated in STAD compared with normal tissues, it was significantly higher in stages 2–4 versus stage 1 disease (Figure 3B). Similarly, grade 3 STAD exhibited higher expression of GFRA3 than grade 1 (Figure 3C). The results of this analysis suggested that GFRA3 is associated with the progression of STAD.

GSEA of GFRA3 in the pan-cancer setting. We sought to determine the role of GFRA3 in different types of cancer. To this end, GSEA was performed to compare the functional status of different biological processes in the pan-cancer

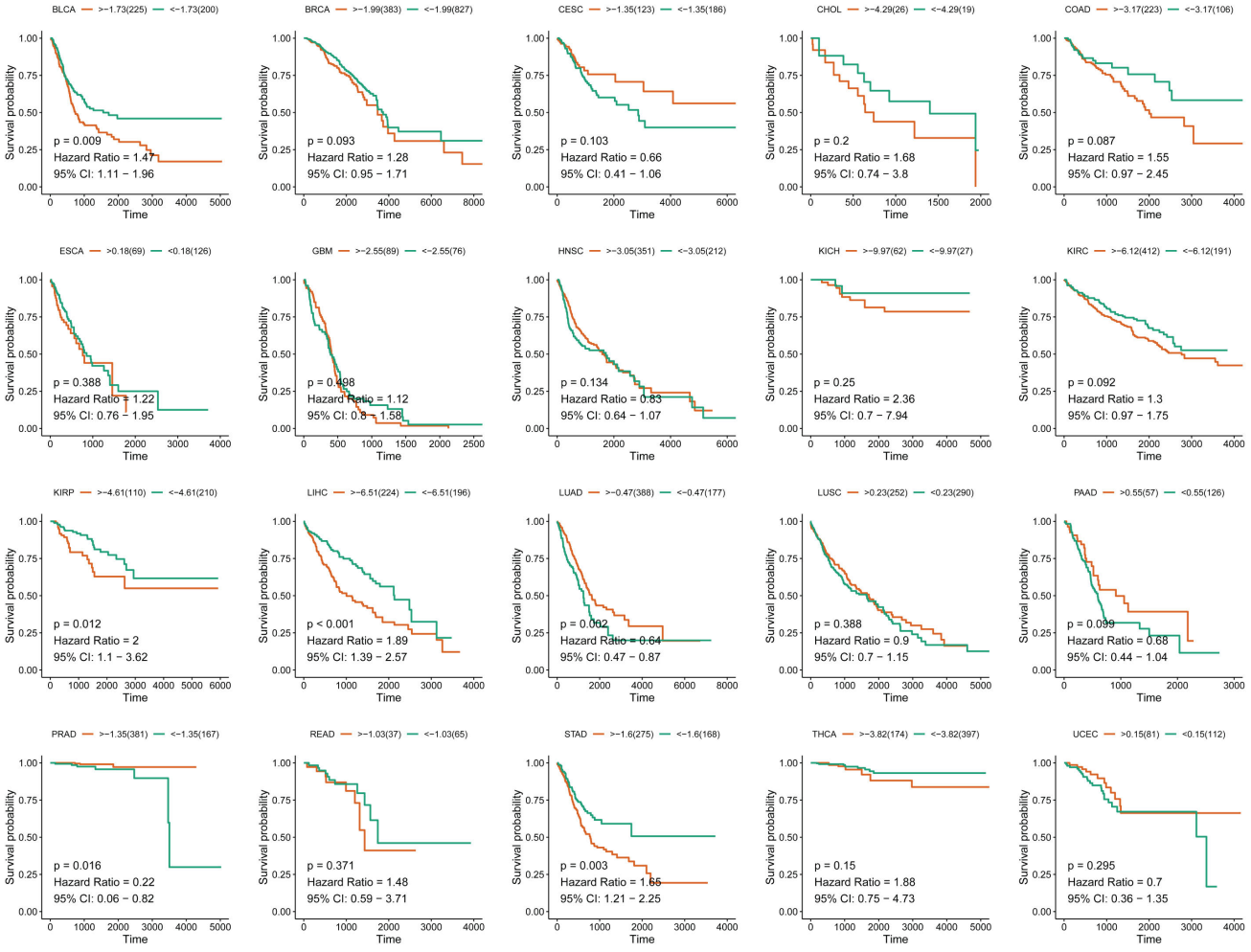

Figure 1. The overall survival (OS) curve of GFRA3 in pan-cancer (a variety of tumor types) (Log-rank test). The horizontal axis is the survival time (day), and the vertical axis is the survival ratio. The red indicates the high GFRA3 expression group, and the green indicates the low GFRA3 expression group.

setting with low and high GFRA3 expression. It was found that the activation status of different processes was highly heterogeneous in different cancer types (Figure 4A). For example, in cancer of the digestive system (i.e., COAD, READ, and STAD), most biological processes were activated when GFRA3 was highly expressed. However, in CESC, glioblastoma, and LUAD, most processes were inhibited with high expression of GFRA3. It was observed that two cancer-associated pathways, namely KRAS signaling and EMT, were activated in most types of cancer. Therefore, the activities of these two pathways were compared in paired tumor and adjacent tissues. The results showed that the activation levels of KRAS_SIGNALING_UP and EMT were higher in STAD tissues versus adjacent tissues. Notably, KRAS_SIGNALING_DN was downregulated in STAD tissues versus adjacent tissues (Figure 4B). Therefore, it was hypothesized that GFRA3 could promote KRAS signaling and EMT in gastric cancer.

GFRA3 promoted the migration and invasion of gastric cancer cells. The expression of GFRA3 was significantly higher in SGC7901 cells versus BGC823 cells (Figure 5A). Thus, GFRA3 was overexpressed and knocked down in BGC823 and SGC7901 cells, respectively. As shown in Figures 5B and 5C, overexpression of GFRA3 slightly increased the viability of BGC823 cells, while knockdown of GFRA3 decreased the viability of SGC7901 cells to some degree. Further studies revealed that overexpression of GFRA3 induced the migration and invasion of BGC823 cells, while knockdown of GFRA3 suppressed these processes in SGC7901 cells (Figures 5D–5G). These findings suggested that GFRA3 promoted the migration and invasion of gastric cancer cells.

GFRA3 activated KRAS downstream signaling and induced EMT in gastric cancer cells. The GSEA data suggested that KRAS signaling activation was related to the high expression of GFRA3 in gastric cancer. Thus, the

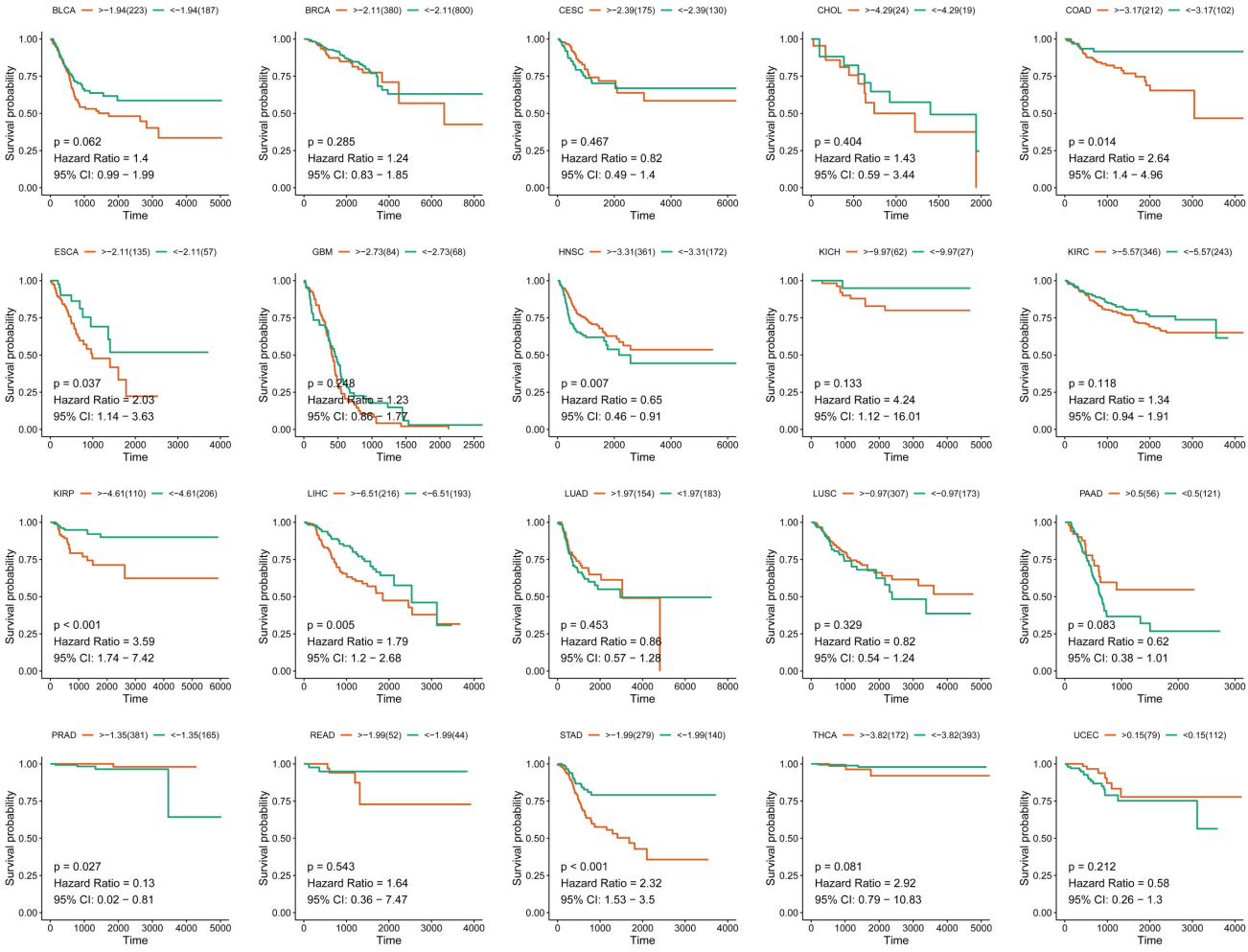

Figure 2. The disease-free survival (DFS) curve of GFRA3 in pan-cancer (a variety of tumor types) (Log-rank test). The horizontal axis is the survival time (day), the vertical axis is the survival ratio, the red indicates the high expression group, and the green indicates the low expression group.

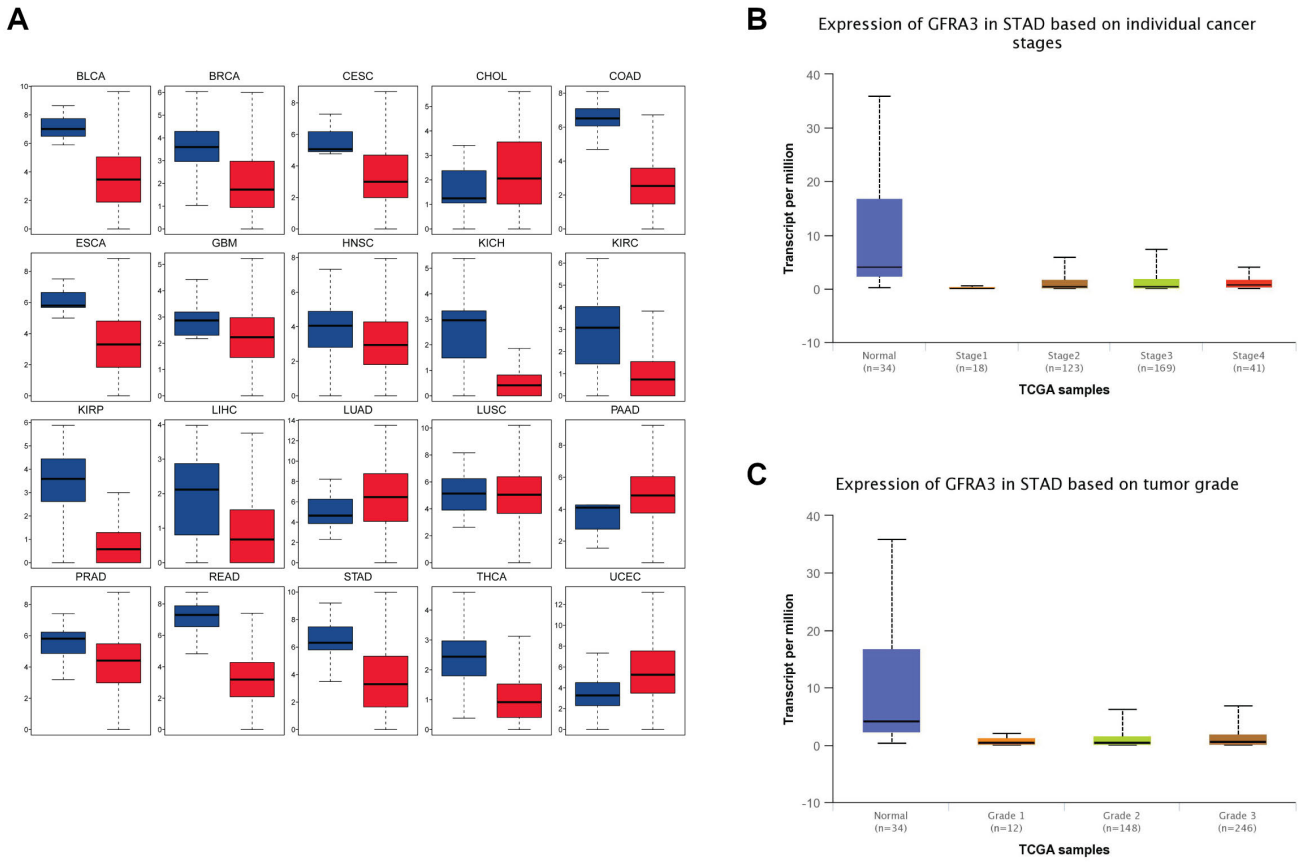

Figure 3. Expression analysis of GFRA3 in STAD dataset. A) The expression of GFRA3 in different datasets from TCGA database. The blue and red indicate normal tissue and tumor tissue, respectively. B, C) Effects of cancer stage (B) and grade (C) on the expression level of GFRA3 in STAD tissues from the TCGA database and analyzed by UALCAN (http://ualcan.path.uab.edu/analysis.html)

involvement of KRAS downstream signaling targets p-AKT and p-ERK was investigated. Overexpression of GFRA3 increased the active KRAS (interacting with RAF-1) and the phosphorylation of AKT and ERK in BGC823 cells. However, the knockdown of GFRA3 exerted an opposite effect in SGC7901 cells (Figures 6A, 6B). In addition, overexpression of GFRA3 downregulated the expression of epithelial markers E-cadherin and ZO-1, whereas it upregulated the levels of mesenchymal markers VIM and FN in BGC823 cells (Figure 6C). Knockdown of GFRA3 induced E-cadherin and ZO-1 expression and reduced VIM and FN expression in SGC7901 cells (Figure 6D). The above results indicated that GFRA3 activated KRAS as well as its downstream AKT and ERK signaling, and induced EMT in gastric cancer cells.

ARTN induced EMT, migration, and invasion of gastric cancer cells via GFRA3/KRAS signaling. GFRA3 belongs to the GDNF receptor family. Hence, it is necessary to clarify whether ARTN activates KRAS signaling through GFRA3. In this study, it was found that ARTN induced the activation of KRAS, as well as the phosphorylation of AKT and ERK. Moreover, following treatment of BGC823 and SGC7901 cells with ARTN, the levels of epithelial markers E-cadherin and ZO-1 were decreased, whereas those of mesenchymal markers VIM and FN were increased. However, the knockdown of GFRA3 attenuated the ARTN-induced activation of KRAS, phosphorylation of AKT and ERK, and EMT (Figures 7A, 7B). Consistently, ARTN promoted the migration and invasion of BGC823 and SGC7901 cells; notably, this effect was inhibited by GFRA3 knockdown (Figures 8A, 8B). To determine whether KRAS mediates the role of ARTN/GFRA3, the activation of KRAS was blocked using BAY-293. In the presence of ARTN, overexpression of GFRA3 increased the levels of active KRAS, p-AKT, p-ERK, and EMT markers in BGC823 and SGC7901 cells. Blockage of KRAS activation by BAY-293 reduced the GFRA3-mediated phosphorylation of AKT and ERK, as well as EMT (Figures 7C, 7D). In the phenotype experiments, the migration and invasion of BGC823 and SGC7901 cells were induced by overexpression of GFRA3; this effect was diminished by treatment with BAY-293 (Figures 8C, 8D). Therefore, these findings suggested that ARTN induced EMT, migration, and invasion of gastric cancer cells via GFRA3/KRAS signaling.

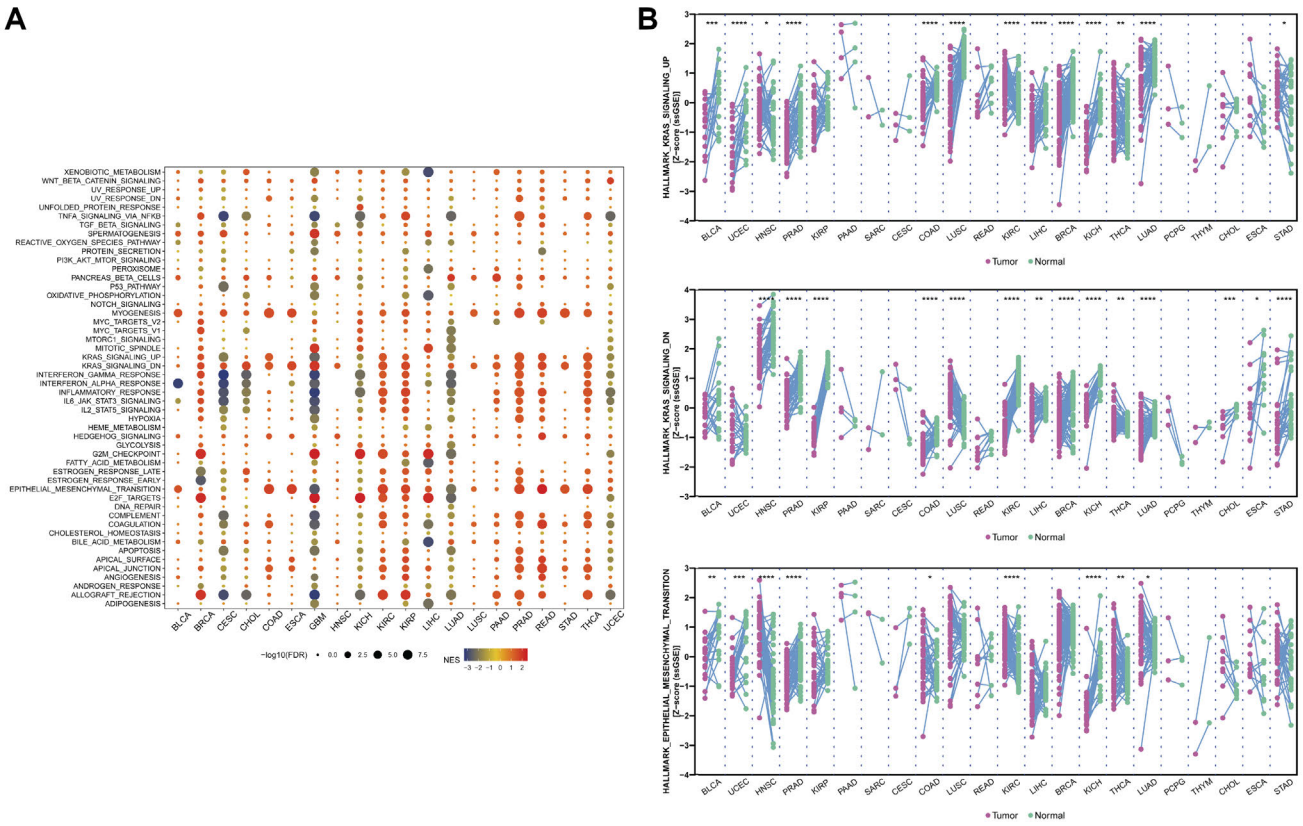

Figure 4. GSEA analysis of GFRA3 in pan-cancer. A) Each row represents a GSEA pathway, each column represents a cancer type, and red and blue represent activation and inhibition status, respectively. B) The activities of KRAS_SIGNALING_UP, KRAS_SIGNALING_DN, and EPITHELIAL_MESENCHYMAL_TRANSITION were compared in the paired sample data (tumor tissue and adjacent tissue) from each cancer type.

High expression of GFRA3 was correlated with the progression of gastric cancer. Immunohistochemical staining was applied to examine the expression of GFRA3 in gastric cancer tissues. GFRA3 expression differed between cases of gastric cancer (Figure 9). Clinical analyses showed that high immunohistochemistry scores of GFRA3 were associated with larger tumor size and advanced TNM stage of gastric cancer (Table 2). These data suggested that high expression of GFRA3 may indicate a poor prognosis for patients with gastric cancer.

Discussion

Previous studies have revealed that high expression of GFRA3 is associated with malignant phenotypes of various tumors. In breast cancer, elevated GFRA3 expression is associated with lymph node metastasis and advanced tumor stage [9]. In pancreatic ductal adenocarcinoma and urothelial cancer, GFRA3 may promote tumor metastasis by enhancing cell migration and invasion [10, 18]. Of note, the expression of GFRA3 is also upregulated in non-small cell lung cancer [19]. However, the pan-cancer analysis in the present study showed that the relationship between GFRA3 expression and prognosis was quite different in diverse cancer types. Thereinto, we found that high expression levels of GFRA3 were strongly associated with both shorter OS and DFS in patients with gastric cancer, suggesting GFRA3 as a prognostic marker in gastric cancer. In consistency with prognostic data, gastric cancers with advanced stage and grade exhibited higher expression of GFRA3 than those with low stage and grade. However, analysis, using data extracted from TCGA database, showed that the expression of GFRA3 was significantly downregulated in gastric cancer tissues compared with normal gastric tissues. Previous studies have demonstrated that high methylation levels of the GFRA3 gene in gastric cancer tissue can lead to a dismal prognosis; nevertheless, there is no clear association between GFRA3 methylation levels and gene expression [20]. In addition, there is no difference in GFRA3 methylation levels between diffuse and intestinal gastric cancer. Therefore, we hypothesized that GFRA3 performs distinct biological functions in gastric cancer and normal cells, which may depend on the levels of GFRA3 ligands in the microenvironment. GFRA3 gene methylation may affect the prognosis of patients with gastric cancer in a manner independent of GFRA3 expression. Anyway, whether GFRA3 is an oncogene and a thera-

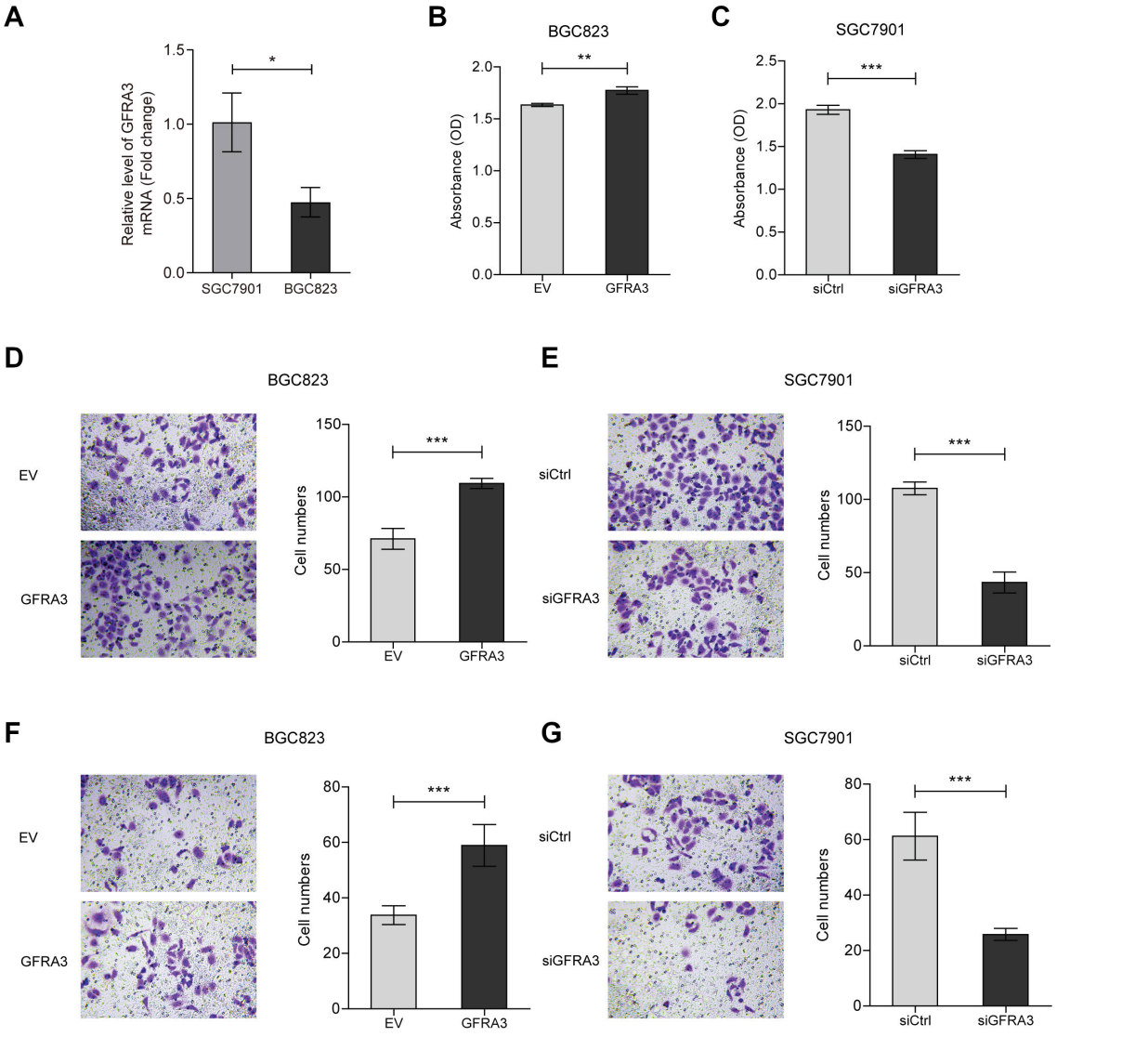

Figure 5. GFRA3 promotes the migration and invasion of gastric cancer cells. A) The mRNA levels of GFRA3 were analyzed by qPCR in SGC7901 and BGC823 cells. B–G) GFRA3 overexpression plasmids and GFRA3 siRNA were transfected into BGC823 and SGC7901 cells for 48 h, respectively. The viability of BGC823 (B) and SGC7901 (C) cells was analyzed by the CCK-8 assay. Representative images of BGC823 (D) and SGC7901 (E) cells migrating to the lower chamber of Transwell in migration assays, and right panels: numbers of migratory cells. Representative images of BGC823 (F) and SGC7901 (G) cells penetrating the Matrigel in invasion assays. and right panels: numbers of invasive cells.

peutic target for gastric cancer still needs to be explored in the future.

The binding of GDNF to GFRA/RET results in the phosphorylation of specific tyrosine residues in the region of RET kinase and subsequent activation of multiple downstream pathways. These pathways include mitogen-activated protein kinase (MAPK), RAS/ERK, PI3K/AKT, SrC-family kinases, phospholipase C gamma (PLC-γ), vav guanine nucleotide exchange factor 2 (Vav-2), and JUN N-terminal kinase (JNK) cascades, which control the differentiation, survival, and function of multiple populations of neurons. In this study, based on GSEA analysis, we found that ARTN activated KRAS signaling in gastric cancer cells through GFRA3, which further activated PI3K/AKT and ERK signaling molecules. Previous studies have found that the activation of KRAS in gastric cancer cells induces EMT and promotes the production of gastric cancer stem cells, thereby facilitating tumor metastasis [21]. In addition, the epidermal growth factor receptor/RAS (EGFR/RAS) pathway, which is essential for the maintenance of gastric stem cells *in vitro* and *in vivo*, is also involved in promoting EMT-induced tumorigenesis [22]. As downstream signaling pathways, KRAS and PI3K/AKT promote EMT in gastric cancer cells by further activating mechanistic target of rapamycin kinase (mTOR),

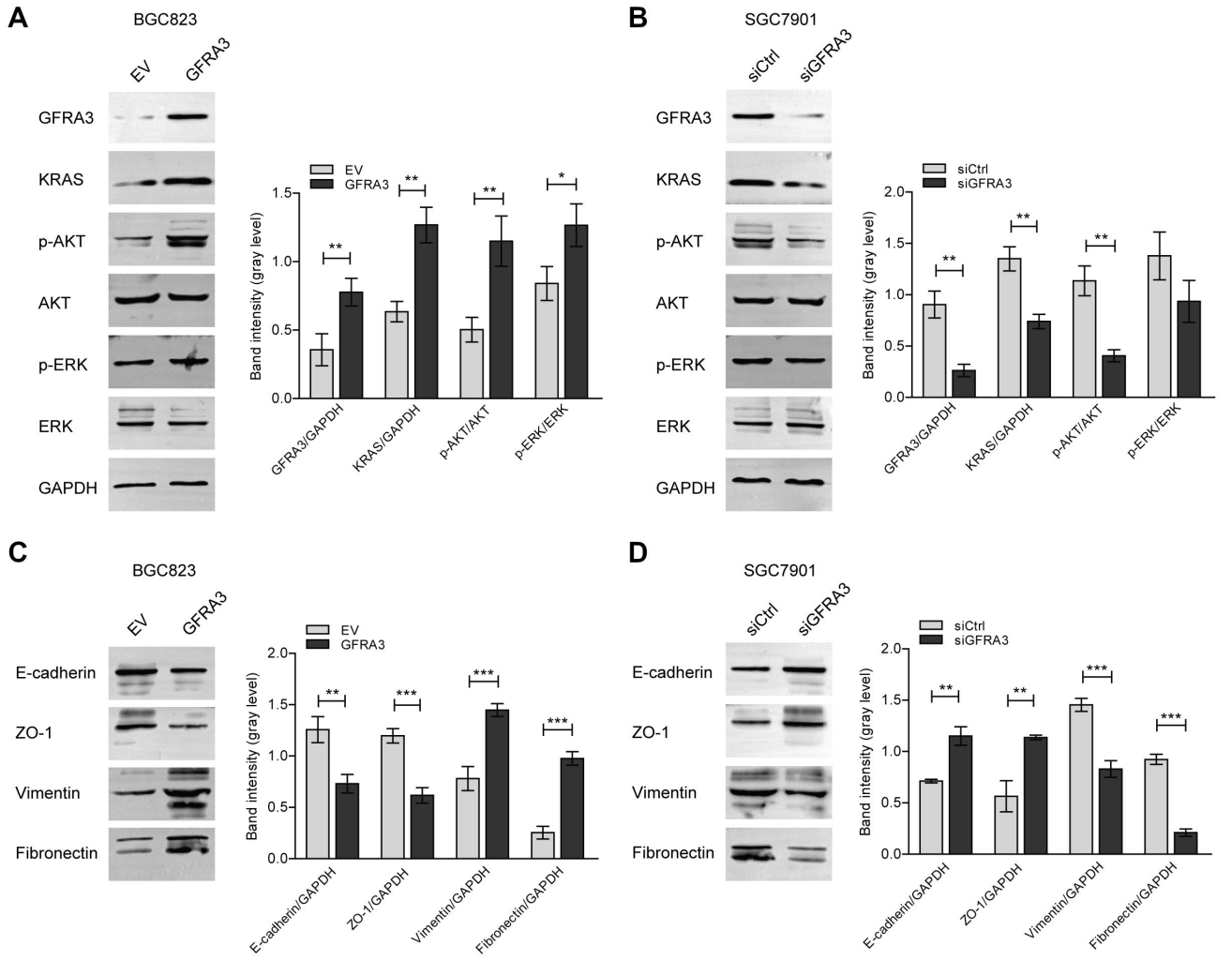

Figure 6. GFRA3 activates KRAS downstream signaling and induces EMT in gastric cancer cells. A, B) GFRA3 overexpression plasmids and GFRA3 siRNAs were transfected into BGC823 and SGC7901 cells for 48 h, respectively. Activated KRAS affinity precipitation assay was performed. The protein levels of KRAS, p-AKT, AKT, p-ERK, and ERK were analyzed by western blot in BGC823 and SGC7901 cells. Right panels: band intensity of the indicated proteins. C, D) The protein levels of E-cadherin, ZO-1, Vimentin, and Fibronectin were analyzed by western blot in BGC823 and SGC7901 cells. Right panels: band intensity of the indicated proteins.

nuclear factor-kappa B (NF-κB), and glycogen synthase kinase-3 beta (GSK-3β) [23–25]. Other studies showed that inhibition of the RAS/RAF1/ERK signaling pathway reduces the EMT phenotype of gastric cancer cells [26, 27]. Interestingly, AKT and ERK are usually simultaneously activated during EMT and metastasis of gastric cancer cells [28, 29]. Here, although the PI3K/AKT pathway was not significantly enriched in GSEA analysis, we noticed that the activation of the ARTN-GFRA3 axis induced the phosphorylation of both AKT and KRAS, revealing that the ARTN-GFRA3 axis could activate the signaling molecules AKT and KRAS in gastric cancer. Our study also showed that treatment with a KRAS inhibitor could weaken the EMT phenotype, and inhibit the migration and invasion of gastric cancer cells. Therefore, it can be inferred that KRAS, as an upstream signaling molecule, plays an important role in the EMT process of gastric cancer cells, which is activated by the ARTN-GFRA3 axis. Notably, in addition to the phenotype EMT, myogenesis was observably activated when GFRA3 was highly expressed in gastric cancer. A recent study reported that enhanced myogenesis of gastric cancer is closely related to enriched gene sets associated with initiation of metastasis, increased EMT, and worse prognosis [30]. Therefore, as a phenotype derived from mesoderm, myogenesis may be induced by the ARTN-GFRA3 axis, which also reflects and influences the activity of EMT in gastric cancer.

The outcomes of a meta-analysis suggested that E-cadherin expression is an important predictor of poor prognosis in Asian patients with gastric cancer [31]. E-cadherin plays a crucial role in cell–cell connection, and the associated

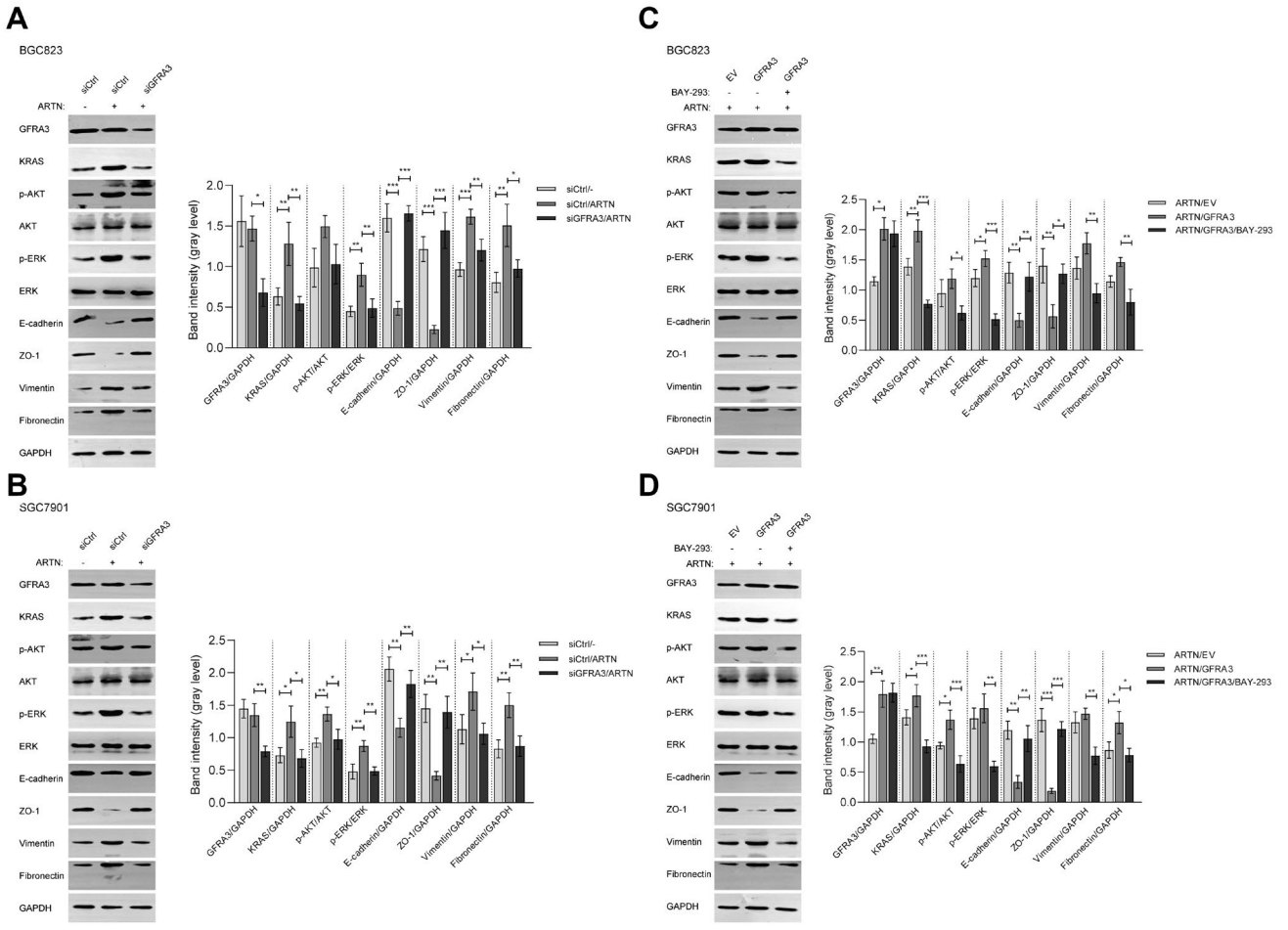

Figure 7. ARTN induces the EMT of gastric cancer cells via GFRA3/KRAS signaling. A, B) GFRA3 siRNAs were transfected into BGC823 and SGC7901 cells treated with 20 ng/ml ARTN for 48 h. Activated KRAS affinity precipitation assay was performed. The protein levels of KRAS, p-AKT, AKT, p-ERK, ERK, E-cadherin, ZO-1, Vimentin, and Fibronectin were analyzed by western blot in BGC823 and SGC7901 cells. Right panels: band intensity of the indicated proteins. C, D) GFRA3 overexpression plasmids were transfected into BGC823 and SGC7901 cells treated with 20 ng/ml ARTN and 50 nM BAY-293 for 48 h. Activated KRAS affinity precipitation assay was performed. The protein levels of KRAS, p-AKT, AKT, p-ERK, ERK, E-cadherin, ZO-1, Vimentin, and Fibronectin were analyzed by western blot in BGC823 and SGC7901 cells. Right panels: band intensity of the indicated proteins.

Table 2. Correlation of the expression of GFRA3 with clinicopathological features in gastric cancer.

		cases	GFRA3 expression				p-value
			–	+	++	+++	
		178	**4**	**22**	**91**	**61**	
Gender							0.6043
	Male	121	2	14	63	42	
	Female	57	2	8	28	19	
Age							0.8713
	≤65	87	3	11	43	30	
	>65	91	1	11	48	31	
Tumor size							0.0406*
	<5 cm	85	4	10	48	23	
	≥5 cm	93	0	12	43	38	
T staging							0.0802
	T1	21	0	5	12	4	
	T2	27	2	2	16	7	
	T3	77	1	11	39	26	
	T4	53	1	4	24	24	
N staging							0.0325*
	N0	49	2	8	25	14	
	N1	36	1	5	22	8	
	N2	36	0	6	19	11	
	N3	57	1	3	25	28	
M staging							0.0037**
	M0	168	4	22	89	53	
	M1	10	0	0	2	8	
TNM							0.0048**
	I	33	2	6	20	5	
	II	48	0	6	26	16	
	III	87	2	10	43	32	
	IV	10	0	0	2	8	

Notes: *p<0.05; **p<0.005

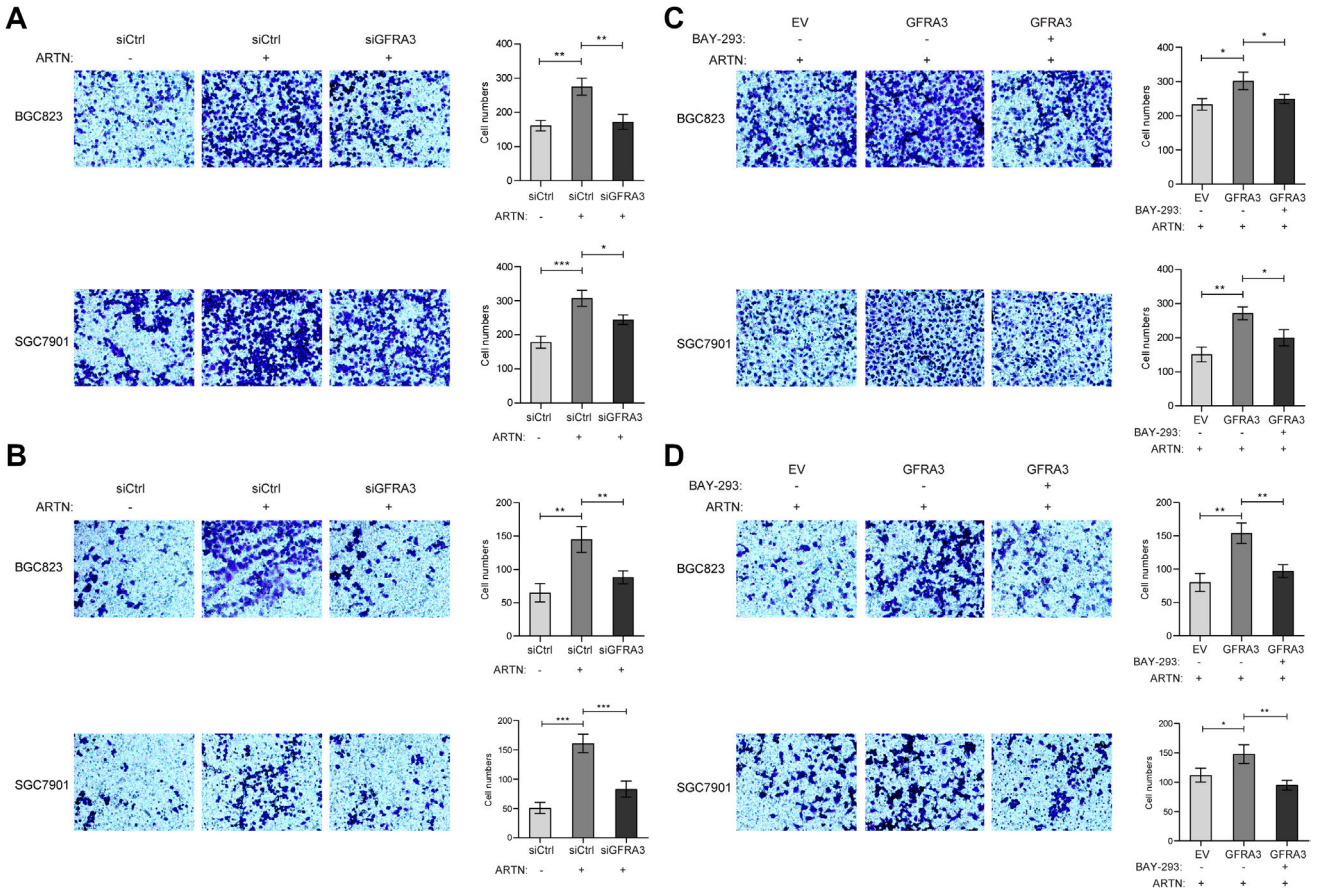

Figure 8. ARTN induces the migration and invasion of gastric cancer cells via GFRA3/KRAS signaling. A, B) GFRA3 siRNAs were transfected into BGC823 and SGC7901 cells treated with 20 ng/ml ARTN for 48 h. Representative images of BGC823 and SGC7901 (A) cells migrating to the lower chamber of Transwell in migration assays, and right panels: numbers of migratory cells. Representative images of BGC823 and SGC7901 (B) cells penetrating the Matrigel in invasion assays, and right panels: numbers of invasive cells. C, D) GFRA3 overexpression plasmids were transfected into BGC823 and SGC7901 cells treated with 20 ng/ml ARTN and 50 nM BAY-293 for 48 h. Representative images of BGC823 and SGC7901 (C) cells migrating to the lower chamber of Transwell in migration assays, and right panels: numbers of migratory cells. Representative images of BGC823 and SGC7901 (D) cells penetrating the Matrigel in invasion assays, and right panels: numbers of invasive cells.

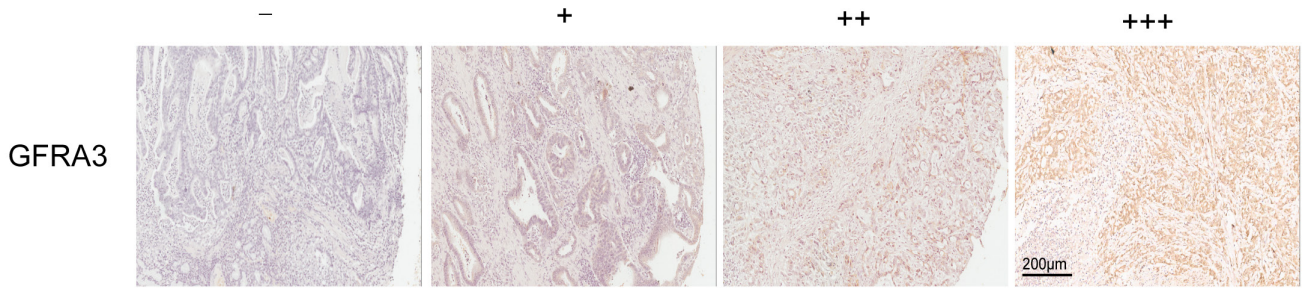

Figure 9. Representative images of GFRA3 staining in gastric cancer tissues. The cases of gastric cancer with different levels of GFRA3.

signaling pathways regulate the fate and inflammation of gastric mucosal epithelial cells. Hence, the inactivation of E-cadherin is critical in the development and progression of gastric cancer [32]. Low expression or absence of E-cadherin is associated with the development of gastric cancer, particularly diffuse gastric cancer. The molecular mechanisms underlying this process involve a variety of aspects, including promoter hypermethylation, somatic and germline mutations, and transcriptional inhibition [31]. ZO-1 is a scaffolding component in the assembly of tight junctions, inhibiting tumor metastasis. ZO-1 expression is significantly decreased in tumors with undifferentiated-type gastric

adenocarcinoma [33]. Our investigation showed that the ARTN-GFRA3 axis inhibited the expression of E-cadherin and ZO-1 through KRAS signaling. According to previous studies, PI3K/AKT and ERK downstream of KRAS may activate the transcriptional inhibitors of E-cadherin (e.g., Snail and Slug), leading to the downregulation of E-cadherin in gastric cancer [34, 35]. In addition, we found that the ARTN-GFRA3 axis could induce the expression of interstitial markers VIM and FN in gastric cancer cells.

VIM is a key indicator of EMT, which promotes cell movement and invasion. Increased VIM expression is associated with diffuse gastric cancer, lymph node invasion and metastasis, and poor prognosis [36]. Previous studies have found that circulating VIM-positive gastric cancer cells are present in the bone marrow of patients with gastric cancer. The expression levels of VIM in the bone marrow are also significantly linked to the abilities of gastric cancer cells for invasion and lymph node metastasis [37]. Extracellular matrix remodeling is a necessary biological process that accelerates the spread of tumor cells during EMT. FN is distributed on the cell surface and extracellular matrix in the form of dimers or polymers, and is involved in cell adhesion and migration during tumor metastasis [38]. Recent studies have shown that the knockdown of FN can impair the migratory and invasive capabilities of gastric cancer cells, and high expression of FN is associated with a poor prognosis in patients with gastric cancer [39]. As presented in the results of our study, increased expression of VIM and FN indicated the EMT progress of gastric cancer when the ARTN-GFRA3 axis was activated.

In summary, this study suggested a potential mechanism for neural invasion in gastric cancer, which was driven by the ARTN-GFRA3 axis. The ARTN-GFRA3 axis promoted the EMT, migration, and invasion of gastric cancer cells via KRAS signaling. TCGA and pathological analyses showed that high expression of GFRA3 was associated with poor prognosis and advanced TNM stage in gastric cancer, respectively.

References

[1] SUNG H, FERLAY J, SIEGEL RL, LAVERSANNE M, SOERJOMATARAM I et al.Global Cancer Statistics 2020: GLOBOCAN Estimates of Incidence and Mortality Worldwide for 36 Cancers in 185 Countries. CA Cancer J Clin 2021; 71: 209–249. https://doi.org/10.3322/caac.21660

[2] ZHAO B, LV W, MEI D, LUO R, BAO S et al. Perineural invasion as a predictive factor for survival outcome in gastric cancer patients: a systematic review and meta-analysis. J Clin Pathol 2020; 73: 544–551. https://doi.org/10.1136/jclinpath-2019-206372

[3] LIEBIG C, AYALA G, WILKS JA, BERGER DH, ALBO D. Perineural invasion in cancer: a review of the literature. Cancer 2009; 115: 3379–3391. https://doi.org/10.1002/cncr.24396

[4] CRIPPA S, PERGOLINI I, JAVED AA, HONSELMANN KC, WEISS MJ et al. Implications of Perineural Invasion on Disease Recurrence and Survival After Pancreatectomy for Pancreatic Head Ductal Adenocarcinoma. Ann Surg 2022; 276: 378–385. https://doi.org/10.1097/SLA.0000000000004464

[5] WEI T, ZHANG XF, HE J, POPESCU I, MARQUES HP et al. Prognostic impact of perineural invasion in intrahepatic cholangiocarcinoma: multicentre study. Br J Surg 2022; 109: 610–616. https://doi.org/10.1093/bjs/znac098

[6] WOODHAM BL, CHMELO J, DONOHOE CL, MADHAVAN A, PHILLIPS AW. Prognostic Significance of Lymphatic, Venous and Perineural Invasion After Neoadjuvant Chemotherapy in Patients with Gastric Adenocarcinoma. Ann Surg Oncol 2020; 27: 3296–3304. https://doi.org/10.1245/s10434-020-08389-7

[7] BAUDET C, MIKAELS A, WESTPHAL H, JOHANSEN J, JOHANSEN TE et al. Positive and negative interactions of GDNF, NTN and ART in developing sensory neuron subpopulations, and their collaboration with neurotrophins. Development 2000; 127: 4335–4344. https://doi.org/10.1242/dev.127.20.4335

[8] ESSEGHIR S, TODD SK, HUNT T, POULSOM R, PLAZA-MENACHO I et al. A role for glial cell derived neurotrophic factor induced expression by inflammatory cytokines and RET/GFR alpha 1 receptor up-regulation in breast cancer. Cancer Res 2007; 67: 11732–11741. https://doi.org/10.1158/0008-5472.CAN-07-2343

[9] WU ZS, PANDEY V, WU WY, YE S, ZHU T et al. Prognostic significance of the expression of GFRalpha1, GFRalpha3 and syndecan-3, proteins binding ARTEMIN, in mammary carcinoma. BMC Cancer 2013; 13: 34. https://doi.org/10.1186/1471-2407-13-34

[10] YAN Y, LI MN, YANG B, GENG J, ZHENG JH et al. Expression of GFRalpha3 correlates with tumor progression and promotes cell metastasis in urothelial carcinoma. Minerva Urol Nefrol 2018; 70: 79–86. https://doi.org/10.23736/S0393-2249.17.02887-9

[11] ZHU DL, LUO DL, LUO G, WANG B, GAO JM. [Artemin and GFRalpha3 expressions and their relevance to perineural invasiveness and metastasis of pancreatic carcinoma]. Nan Fang Yi Ke Da Xue Xue Bao 2009; 29: 428–432.

[12] DAS V, BHATTACHARYA S, CHIKKAPUTTAIAH C, HAZRA S, PAL M. The basics of epithelial-mesenchymal transition (EMT): A study from a structure, dynamics, and functional perspective. J Cell Physiol 2019; 234:14535–14555. https://doi.org/10.1002/jcp.28160

[13] PENG Z, WANG CX, FANG EH, WANG GB, TONG Q. Role of epithelial-mesenchymal transition in gastric cancer initiation and progression. World J Gastroenterol 2014; 20: 5403–5410. https://doi.org/10.3748/wjg.v20.i18.5403

[14] HUANG L, WU RL, XU AM. Epithelial-mesenchymal transition in gastric cancer. Am J Transl Res 2015; 7: 2141–2158.

[15] YILMAZ M, CHRISTOFORI G. EMT, the cytoskeleton, and cancer cell invasion. Cancer Metastasis Rev 2009; 28: 15–33. https://doi.org/10.1007/s10555-008-9169-0

[16] ZHENG HX, CAI Y D, WANG YD, CUI XB, XIE TT et al. Fas signaling promotes motility and metastasis through epithelial-mesenchymal transition in gastrointestinal cancer. Oncogene 2013; 32: 1183–1192. https://doi.org/10.1038/onc.2012.126

[17] OH SC, SOHN BH, CHEONG JH, KIM SB, LEE JE et al.Clinical and genomic landscape of gastric cancer with a mesenchymal phenotype. Nat Commun 2018; 9: 1777. https://doi.org/10.1038/s41467-018-04179-8

[18] LI TJ, LI H, ZHANG WH, XU SS, JIANG W et al. Human splenic TER cells: A relevant prognostic factor acting via the artemin-GFRalpha3-ERK pathway in pancreatic ductal adenocarcinoma. Int J Cancer 2021; 148: 1756–1767. https://doi.org/10.1002/ijc.33410

[19] TANG JZ, KONG XJ, KANG J, FIELDER GC, STEINER M et al. Artemin-stimulated progression of human non-small cell lung carcinoma is mediated by BCL2. Mol Cancer Ther 2010; 9: 1697–1708. https://doi.org/10.1158/1535-7163.MCT-09-1077

[20] EFTANG LL, KLAJIC J, KRISTENSEN VN, TOST J, ESBENSEN QY et al. GFRA3 promoter methylation may be associated with decreased postoperative survival in gastric cancer. BMC Cancer 2016; 16: 225. https://doi.org/10.1186/s12885-016-2247-8

[21] YOON C, TILL J, CHO SJ, CHANG KK, LIN JX et al. KRAS Activation in Gastric Adenocarcinoma Stimulates Epithelial-to-Mesenchymal Transition to Cancer Stem-Like Cells and Promotes Metastasis. Mol Cancer Res 2019; 17: 1945–1957. https://doi.org/10.1158/1541-7786.MCR-19-0077

[22] VOON DC, WANG H, KOO JK, CHAI JH, HOR YT et al.EMT-induced stemness and tumorigenicity are fueled by the EGFR/Ras pathway. PLoS One 2013; 8: e70427. https://doi.org/10.1371/journal.pone.0070427

[23] WANG C, YANG Z, XU E, SHEN X, WANG X et al. Apolipoprotein C-II induces EMT to promote gastric cancer peritoneal metastasis via PI3K/AKT/mTOR pathway. Clin Transl Med 2021; 11: e522. https://doi.org/10.1002/ctm2.522

[24] CHEN H, JIANG T, CHEN H, SU J, WANG X et al. Brusatol reverses lipopolysaccharide-induced epithelial-mesenchymal transformation and induces apoptosis through PI3K/Akt/NF-small ka, CyrillicB pathway in human gastric cancer SGC-7901 cells. Anticancer Drugs 2021; 32: 394–404. https://doi.org/10.1097/CAD.0000000000001022

[25] GE H, LIANG C, LI Z, AN D, REN S et al. DcR3 induces proliferation, migration, invasion, and EMT in gastric cancer cells via the PI3K/AKT/GSK-3beta/beta-catenin signaling pathway. Onco Targets Ther 2018; 11: 4177–4187. https://doi.org/10.2147/OTT.S172713

[26] GE P, WEI L, ZHANG M, HU B, WANG K et al. TRPC1/3/6 inhibition attenuates the TGF-beta1-induced epithelial-mesenchymal transition in gastric cancer via the Ras/Raf1/ERK signaling pathway. Cell Biol Int 2018; 42: 975–984. https://doi.org/10.1002/cbin.10963

[27] WANG C, REN C, HU Q, SHEN X, WANG M et al. Histidine-rich calcium binding protein promotes gastric cancer cell proliferation, migration, invasion and epithelial-mesenchymal transition through Raf/MEK/ERK signaling. J Cancer 2022; 13: 1073–1085. https://doi.org/10.7150/jca.68403

[28] PEI YF, ZHANG YJ, LEI Y, WU WD, MA TH et al. Hypermethylation of the CHRDL1 promoter induces proliferation and metastasis by activating Akt and Erk in gastric cancer. Oncotarget 2017; 8: 23155–23166. https://doi.org/10.18632/oncotarget.15513

[29] LIAO A, WANG W, SUN D, JIANG Y, TIAN S et al. Bone morphogenetic protein 2 mediates epithelial-mesenchymal transition via AKT and ERK signaling pathways in gastric cancer. Tumour Biol 2015; 36: 2773–2778. https://doi.org/10.1007/s13277-014-2901-1

[30] CHIDA K, OSHI M, AN N, KANAZAWA H, ROY A M et al. Gastric cancer with enhanced myogenesis is associated with less cell proliferation, enriched epithelial-to-mesenchymal transition and angiogenesis, and poor clinical outcomes. Am J Cancer Res 2024; 14: 355–367. https://doi.org/10.62347/NCIM3072

[31] XING X, TANG YB, YUAN G, WANG Y, WANG J et al. The prognostic value of E-cadherin in gastric cancer: a meta-analysis. Int J Cancer 2013; 132: 2589–2596. https://doi.org/10.1002/ijc.27947

[32] LIU X, CHU KM. E-cadherin and gastric cancer: cause, consequence, and applications. Biomed Res Int 2014; 2014: 637308. https://doi.org/10.1155/2014/637308

[33] OHTANI S, TERASHIMA M, SATOH J, SOETA N, SAZE Z et al. Expression of tight-junction-associated proteins in human gastric cancer: downregulation of claudin-4 correlates with tumor aggressiveness and survival. Gastric Cancer 2009; 12: 43–51. https://doi.org/10.1007/s10120-008-0497-0

[34] BECKER KF, ROSIVATZ E, BLECHSCHMIDT K, KREMMER E, SARBIA M et al. Analysis of the E-cadherin repressor Snail in primary human cancers. Cells Tissues Organs 2007; 185: 204–212. https://doi.org/10.1159/000101321

[35] ALVES CC, CARNEIRO F, HOEFLER H, BECKER KF. Role of the epithelial-mesenchymal transition regulator Slug in primary human cancers. Front Biosci (Landmark Ed) 2009; 14: 3035–3050. https://doi.org/10.2741/3433

[36] ZHAO Y, YAN Q, LONG X, CHEN X, WANG Y. Vimentin affects the mobility and invasiveness of prostate cancer cells. Cell Biochem Funct 2008; 26: 571–577. https://doi.org/10.1002/cbf.1478

[37] IWATSUKI M, MIMORI K, FUKAGAWA T, ISHII H, YOKOBORI T et al. The clinical significance of vimentin-expressing gastric cancer cells in bone marrow. Ann Surg Oncol 2010; 17: 2526–2533. https://doi.org/10.1245/s10434-010-1041-0

[38] PEIXOTO P, ETCHEVERRY A, AUBRY M, MISSEY A, LACHAT C et al. EMT is associated with an epigenetic signature of ECM remodeling genes. Cell Death Dis 2019; 10: 205. https://doi.org/10.1038/s41419-019-1397-4

[39] LIU YP, CHEN WD, LI WN, ZHANG M. Overexpression of FNDC1 Relates to Poor Prognosis and Its Knockdown Impairs Cell Invasion and Migration in Gastric Cancer. Technol Cancer Res Treat 2019; 18: 1533033819869928. https://doi.org/10.1177/1533033819869928